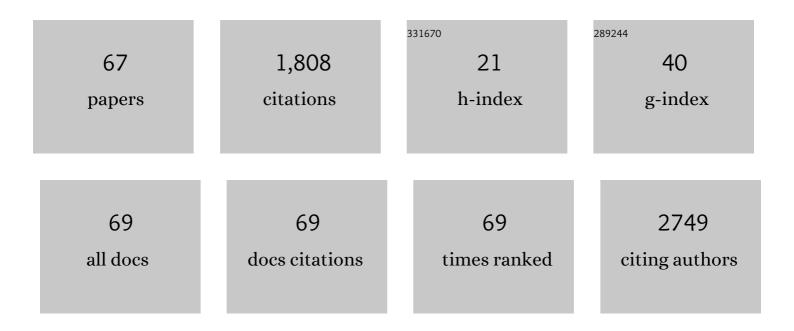
Katarzyna M Marzec

List of Publications by Year in descending order

Source: https://exaly.com/author-pdf/6270797/publications.pdf Version: 2024-02-01



#	Article	IF	CITATIONS
1	Temporal relationship between systemic endothelial dysfunction and alterations in erythrocyte function in a murine model of chronic heart failure. Cardiovascular Research, 2022, 118, 2610-2624.	3.8	17
2	Trends in biomedical analysis of red blood cells – Raman spectroscopy against other spectroscopic, microscopic and classical techniques. TrAC - Trends in Analytical Chemistry, 2022, 146, 116481.	11.4	15
3	Sex-Specific Differences of Adenosine Triphosphate Levels in Red Blood Cells Isolated From ApoE/LDLR Double-Deficient Mice. Frontiers in Physiology, 2022, 13, 839323.	2.8	1
4	Probing Heme Active Sites of Hemoglobin in Functional Red Blood Cells Using Resonance Raman Spectroscopy. Journal of Physical Chemistry B, 2021, 125, 3556-3565.	2.6	7
5	An Insight into the Stages of Ion Leakage during Red Blood Cell Storage. International Journal of Molecular Sciences, 2021, 22, 2885.	4.1	6
6	Spectroscopic Signature of Red Blood Cells in a D-Galactose-Induced Accelerated Aging Model. International Journal of Molecular Sciences, 2021, 22, 2660.	4.1	9
7	Tauroursodeoxycholic Acid (TUDCA)—Lipid Interactions and Antioxidant Properties of TUDCA Studied in Model of Photoreceptor Membranes. Membranes, 2021, 11, 327.	3.0	3
8	High-Resolution Fourier Transform Infrared (FT-IR) Spectroscopic Imaging for Detection of Lung Structures and Cancer-Related Abnormalities in a Murine Model. Applied Spectroscopy, 2021, , 000370282110255.	2.2	2
9	Sex-dependent membranopathy in stored human red blood cells. Haematologica, 2021, 106, 2779-2782.	3.5	9
10	Fall in the ATP levels in the red blood cells in ApoE-LDLR double-deficient mice model prior to atherosclerosis development. European Heart Journal, 2021, 42, .	2.2	0
11	Towards Raman-Based Screening of Acute Lymphoblastic Leukemia-Type B (B-ALL) Subtypes. Cancers, 2021, 13, 5483.	3.7	9
12	Tracking Extracellular Matrix Remodeling in Lungs Induced by Breast Cancer Metastasis. Fourier Transform Infrared Spectroscopic Studies. Molecules, 2020, 25, 236.	3.8	12
13	Multimodal detection and analysis of a new type of advanced Heinz body-like aggregate (AHBA) and cytoskeleton deformation in human RBCs. Analyst, The, 2020, 145, 1749-1758.	3.5	6
14	Irreversible alterations in the hemoglobin structure affect oxygen binding in human packed red blood cells. Biochimica Et Biophysica Acta - Molecular Cell Research, 2020, 1867, 118803.	4.1	15
15	Age–related and atherosclerosis–related erythropathy in ApoE/LDLRâ^'/â^' mice. Biochimica Et Biophysica Acta - Molecular Basis of Disease, 2020, 1866, 165972.	3.8	14
16	Temporal sequence of the human RBCs' vesiculation observed in nano-scale with application of AFM and complementary techniques. Nanomedicine: Nanotechnology, Biology, and Medicine, 2020, 28, 102221.	3.3	11
17	Probing the structure-function relationship of hemoglobin in living human red blood cells. Spectrochimica Acta - Part A: Molecular and Biomolecular Spectroscopy, 2020, 239, 118530.	3.9	13
18	Comparison of standard and HD FT-IR with multimodal CARS/TPEF/SHG/FLIMS imaging in the detection of the early stage of pulmonary metastasis of murine breast cancer. Analyst, The, 2020, 145, 4982-4990.	3.5	5

KATARZYNA M MARZEC

#	Article	IF	CITATIONS
19	Vibrational imaging of proteins: changes in the tissues and cells in the lifestyle disease studies. , 2020, , 177-218.		1
20	Resonance Raman spectroscopy of hemoglobin in red blood cells. , 2020, , 375-414.		4
21	FTIR, Raman and AFM characterization of the clinically valid biochemical parameters of the thrombi in acute ischemic stroke. Scientific Reports, 2019, 9, 15475.	3.3	27
22	An Analysis of Isolated and Intact RBC Membranes—A Comparison of a Semiquantitative Approach by Means of FTIR, Nano-FTIR, and Raman Spectroscopies. Analytical Chemistry, 2019, 91, 9867-9874.	6.5	34
23	High and ultraâ€high definition of infrared spectral histopathology gives an insight into chemical environment of lung metastases in breast cancer. Journal of Biophotonics, 2019, 12, e201800345.	2.3	18
24	Raman Imaging of Biomedical Samples. Springer Series in Surface Sciences, 2018, , 307-346.	0.3	3
25	Parasites under the Spotlight: Applications of Vibrational Spectroscopy to Malaria Research. Chemical Reviews, 2018, 118, 5330-5358.	47.7	40
26	Label-free Raman hyperspectral imaging analysis localizes the cyanogenic glucoside dhurrin to the cytoplasm in sorghum cells. Scientific Reports, 2018, 8, 2691.	3.3	22
27	FT-IR- and Raman-based biochemical profiling of the early stage of pulmonary metastasis of breast cancer in mice. Analyst, The, 2018, 143, 2042-2050.	3.5	23
28	Spectroscopy-based characterization of Hb–NO adducts in human red blood cells exposed to NO-donor and endothelium-derived NO. Analyst, The, 2018, 143, 4335-4346.	3.5	11
29	Diversity among endothelial cell lines revealed by Raman and Fourier-transform infrared spectroscopic imaging. Analyst, The, 2018, 143, 4323-4334.	3.5	5
30	Label-free FTIR spectroscopy detects and visualizes the early stage of pulmonary micrometastasis seeded from breast carcinoma. Biochimica Et Biophysica Acta - Molecular Basis of Disease, 2018, 1864, 3574-3584.	3.8	19
31	Raman imaging of heme metabolism <i>in situ</i> in macrophages and Kupffer cells. Analyst, The, 2018, 143, 3489-3498.	3.5	28
32	Resonance Raman and UVâ€Visible Microscopy Reveals that Conditioning Red Blood Cells with Repeated Doses of Sodium Dithionite Increases Haemoglobin Oxygen Uptake. ChemistrySelect, 2017, 2, 3342-3346.	1.5	9
33	Label-free in vivo Raman microspectroscopic imaging of the macromolecular architecture of oocytes. Scientific Reports, 2017, 7, 8945.	3.3	28
34	Different route of hydroxide incorporation and thermal stability of new type of water clathrate: X-ray single crystal and Raman investigation. Scientific Reports, 2017, 7, 9046.	3.3	5
35	Resonance Raman in Vitro Detection and Differentiation of the Nitrite-Induced Hemoglobin Adducts in Functional Human Red Blood Cells. Journal of Physical Chemistry B, 2016, 120, 12249-12260.	2.6	14
36	Raman spectroscopy as a sensitive probe of soft tissue composition – Imaging of cross-sections of various organs vs. single spectra of tissue homogenates. TrAC - Trends in Analytical Chemistry, 2016, 85, 117-127.	11.4	38

#	Article	IF	CITATIONS
37	IR and Raman imaging of murine brains from control and ApoE/LDLR ^{â^'/â^'} mice with advanced atherosclerosis. Analyst, The, 2016, 141, 5329-5338.	3.5	25
38	Effects of Low Carbohydrate High Protein (LCHP) diet on atherosclerotic plaque phenotype in ApoE/LDLRâ^'/â^' mice: FT-IR and Raman imaging. Scientific Reports, 2015, 5, 14002.	3.3	22
39	Vascular diseases investigated ex vivo by using Raman, FT-IR and complementary methods. Pharmacological Reports, 2015, 67, 744-750.	3.3	15
40	Highâ€resolution Raman imaging reveals spatial location of heme oxidation sites in single red blood cells of dried smears. Journal of Raman Spectroscopy, 2015, 46, 76-83.	2.5	37
41	Comparison of transflection and transmission FTIR imaging measurements performed on differentially fixed tissue sections. Analyst, The, 2015, 140, 2376-2382.	3.5	24
42	Raman microimaging of murine lungs: insight into the vitamin A content. Analyst, The, 2015, 140, 2171-2177.	3.5	18
43	Raman spectroscopic studies of vitamin A content in the liver: a biomarker of healthy liver. Analyst, The, 2015, 140, 2074-2079.	3.5	28
44	Surface enhanced Raman spectroscopy of polycyclic aromatic hydrocarbons and molecular asphaltenes. Chemical Physics Letters, 2015, 620, 139-143.	2.6	22
45	Composition and (in)homogeneity of carotenoid crystals in carrot cells revealed by high resolution Raman imaging. Spectrochimica Acta - Part A: Molecular and Biomolecular Spectroscopy, 2015, 136, 1395-1400.	3.9	19
46	Red Blood Cells Polarize Green Laser Light Revealing Hemoglobin′s Enhanced Nonâ€Fundamental Raman Modes. ChemPhysChem, 2014, 15, 3963-3968.	2.1	28
47	Visualization of the biochemical markers of atherosclerotic plaque with the use of Raman, IR and AFM. Journal of Biophotonics, 2014, 7, 744-756.	2.3	57
48	An impact of the ring substitution in nicorandil on its adsorption on silver nanoparticles. Surface-enhanced Raman spectroscopy studies. Spectrochimica Acta - Part A: Molecular and Biomolecular Spectroscopy, 2014, 129, 624-631.	3.9	5
49	Vapnikite Ca ₃ UO ₆ – a new double-perovskite mineral from pyrometamorphic larnite rocks of the Jabel Harmun, Palestinian Autonomy, Israel. Mineralogical Magazine, 2014, 78, 571-581.	1.4	25
50	Vibrational Microspectroscopy for Analysis of Atherosclerotic Arteries. Challenges and Advances in Computational Chemistry and Physics, 2014, , 505-535.	0.6	2
51	Raman spectroscopy of proteins: a review. Journal of Raman Spectroscopy, 2013, 44, 1061-1076.	2.5	783
52	Pathological changes in the biochemical profile of the liver in atherosclerosis and diabetes assessed by Raman spectroscopy. Analyst, The, 2013, 138, 3885.	3.5	45
53	Vorlanite, (CaU6+)O4, from Jabel Harmun, Palestinian Autonomy, Israel. American Mineralogist, 2013, 98, 1938-1942.	1.9	17
54	Substituent effect on structure and surface activity of Nâ€methylpyridinium salts studied by FTâ€IR, FTâ€RS, SERS and DET calculations, Journal of Raman Spectroscopy, 2013, 44, 155-165	2.5	15

#	Article	IF	CITATIONS
55	Structural characterization of rondorfite, calcium silica chlorine mineral containing magnesium in tetrahedral position [MgO4]6â^', with the aid of the vibrational spectroscopies and fluorescence. Spectrochimica Acta - Part A: Molecular and Biomolecular Spectroscopy, 2013, 101, 382-388.	3.9	12
56	Attenuated total reflection Fourier transform infrared (ATR-FTIR) spectroscopy of a single endothelial cell. Analyst, The, 2012, 137, 4135.	3.5	32
57	Nicotinamide and trigonelline studied with surface-enhanced FT-Raman spectroscopy. Vibrational Spectroscopy, 2012, 63, 469-476.	2.2	14
58	Trabzonite, Ca ₄ [Si ₃ O ₉ (OH)]OH: crystal structure, revised formula, new occurrence and relation to killalaite. Mineralogical Magazine, 2012, 76, 455-472.	1.4	9
59	Comparative Matrix Isolation Infrared Spectroscopy Study of 1,3- and 1,4-Diene Monoterpenes (α-Phellandrene and γ-Terpinene). Journal of Physical Chemistry A, 2011, 115, 4342-4353.	2.5	24
60	Insight into coordination of dilead unit by molecules of 4-thiazolidinone-2-thione: Structural and computational studies. Inorganica Chimica Acta, 2011, 376, 581-589.	2.4	5
61	Interaction between rhodanine and silver species on a nanocolloidal surface and in the solid state. Journal of Raman Spectroscopy, 2010, 41, 543-552.	2.5	22
62	Adsorption Of Rhodanine Derivatives On Silver And Gold Nanoparticle Surfaces. , 2010, , .		0
63	Potential-dependent Characterization of Bombesin Adsorbed on Roughened Ag, Au, and Cu Electrode Surfaces. , 2010, , .		0
64	Vibrational Studies on Conformational Preferences of Terpinene Isomers in the Equilibrium Gas and Condensed Phases. , 2010, , .		0
65	Vibrational Characterization of Binding Model of 4-thiazolidinone-2-thione with Pb[sub 2][sup 2+] species. , 2010, , .		0
66	Identification of Arbuscular Mycorrhizal Fungal (AMF) Spore Components. , 2010, , .		0
67	Conformational Space and Photochemistry of α-Terpinene. Journal of Physical Chemistry A, 2010, 114, 5526-5536.	2.5	18